# Prediction of the tool displacement for robot milling applications using coupled models of an industrial robot and removal simulation

*E. Abele [a.], J. Bauer [a.], M. Pischan [a.], O. v. Stryk [b.], M. Friedmann [b.], T. Hemker [b.]*
*a.) Technische Universität Darmstadt, Germany,*
*Institute of Production Management, Technology and Machine Tools (PTW),*
*Petersenstraße 30, 64287 Darmstadt*
*abele@ptw.tu-darmstadt.de*
*b.) Technische Universität Darmstadt, Germany,*
*Simulation, Systems Optimization and Robotics Group (SIM),*
*Hochschulstraße 10, 64289 Darmstadt*
*stryk@sim.tu-darmstadt.de*

**Abstract:** Industrial robots are used in a great variety of applications for handling, welding and milling operations. They represent a cost-saving and flexible alternative for machining applications. A reduced pose and path accuracy, especially under process force load due to the high mechanical compliance, restrict the use of industrial robots for further machining applications. In this paper a method is presented to predict the resulting path deviation of the robot under process force. A process force simulation based on a material removal calculation is proposed. The presented material removal simulation allows the calculation of the chip geometry even in complex cutter work piece engagement conditions. The removal simulation is validated by means of conducted milling tests. By coupling the removal simulation with a robot model the path deviation can be predicted.

**Keywords**: Milling, Industrial Robot, Machine Process Interaction, Material removal simulation

## 1. INTRODUCTION

The major fields of machining applications for industrial robots are automated pre-machining, deburring and fettling of cast parts or trimming of carbon fiber reinforced laminate. Due to the 6 axis robot a large working space and complex machining operations can be conducted. Therefore, compared to standard machine tools industrial robots offer an economic machining alternative. However, industrial robots do not provide a high absolute and repeat accuracy. Current industrial robot systems reach a repeat accuracy of 0.06 mm and an absolute accuracy of $\pm 0.1 - 0.2$ mm after calibration. Under process load, e.g. in milling operation an additional deflection of the tool center point (TCP) occurs. Due to the high compliance, deflections of 0.25 mm

were measured under process loads of 100 N in earlier tests [Abele, 2008]. Therefore, using an industrial robot for milling applications inaccuracies of the serial robot kinematic, the low structural stiffness as well as the effective process forces lead to path deviations. The results are unwanted trajectory deviations, which lead to errors in dimension and a reduced surface quality of the work piece. These deviations mainly consist of a static offset overlaid with a low frequency oscillation of the tool [Weigold, 2008]. In order to increase the milling accuracy with present process forces this paper presents a method to calculate the deviations in milling operation. While the model of the robot was introduced in [Abele, 2008] the focus of this paper is the process force calculation based on a material removal computation.

## 2. OFFLINE PATH CORRECTION FOR MILLING WITH AN INDUSTRIAL ROBOT

The calculation of the deviation is the basis for the correction of the robot trajectory. In order to calculate the deviation a coupled model is used, consisting of a robot model and a process force calculation to simulate the machine – process interaction (cp. Figure 1).
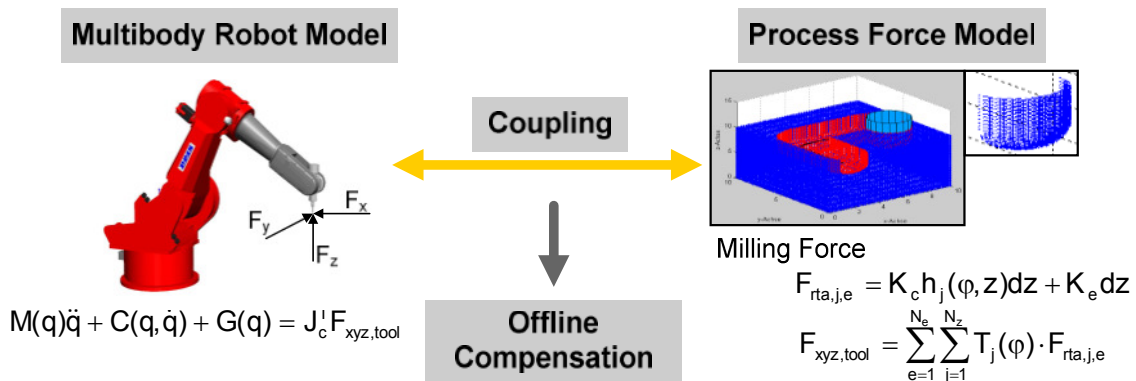


**Multibody Robot Model**

$$M(q)\ddot{q} + C(q,\dot{q}) + G(q) = J_c^! F_{xyz,tool}$$

**Coupling**

**Offline Compensation**

**Process Force Model**

Milling Force

$$F_{rta,j,e} = K_c h_j(\varphi,z)dz + K_e dz$$

$$F_{xyz,tool} = \sum_{e=1}^{N_e} \sum_{j=1}^{N_z} T_j(\varphi) \cdot F_{rta,j,e}$$

*Figure 1; Coupling of the robot with a removal simulation.*

## 3. PROCESS FORCE CALCULATION

The calculation of the milling forces is based on a material removal simulation that can also calculate complex cutter work piece engagement conditions and hence the chip geometry. Based on the chip geometry the milling forces can be calculated using a standard milling force model presented in [Altintas, 2000]. While other methods for cutter work piece engagement simulations are introduced in [Rehling 2009; Surmann, 2005; Selle 2003] the dexel representation offers a simple and fast computation of the engagement condition. Especially, in case of milling with industrial robot the accuracy of this dexel based method for calculating the cutter work piece engagement is considered to be appropriate. In order to increase the calculation accuracy [Weinert,

2002] recommends the usage of a multi dexel volume model for the representation of the work piece for milling applications (cp. Figure 2).
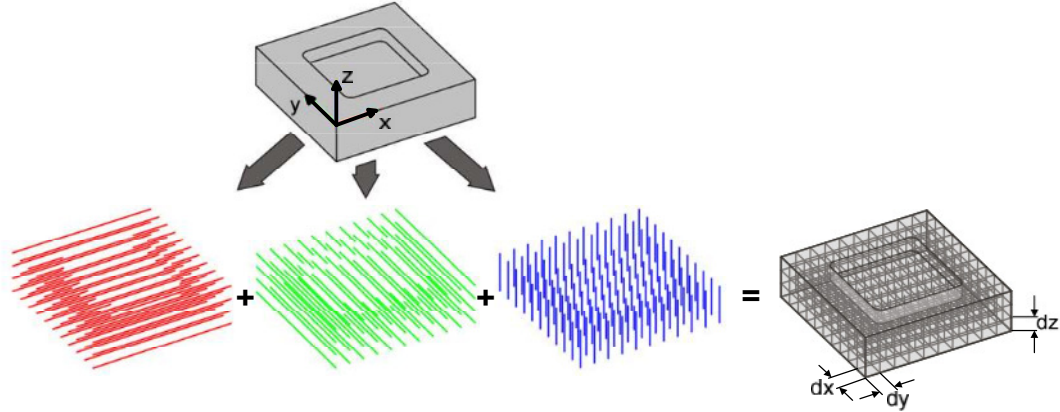


*Figure 2; Dexel representation of a work piece in three directions in space.*

Thereby the description of a single dexel is done by line equations.

$$\bar{p} = \bar{d}t + \bar{s} \tag{1}$$

In Eq. (1) $\bar{p}$ is a point on the line, $\bar{d}$ is the line direction, t is the scaling factor and $\bar{s}$ the starting point in space. The work piece model in this paper is implemented as an orthogonal 3-dexel model. The discretisation of the work piece is defined by the nail distances dx, dy, dz (cp. Figure 2). In order to receive a sufficient accuracy of the force calculation the relation between the dexel discretisation and the tool radius R should be considered

$$k_d = \frac{dx}{R} = \frac{dy}{R} = \frac{dz}{R} = 0,05 \tag{2}$$

During a simulated milling operation the tool moves through the work piece in discrete time steps $t_i$. The incremental size of the time step is the tooth passing time $dt_{tool}$ calculated by

$$dt_{tool} = \frac{n}{N_z \cdot 60} \tag{3}$$

with the number of revolution n and the number of teeth Nz. In each time step $t_i$ the material removal is calculated in the tooth passing time.

### 3.1. Calculation of the chip geometry

The material removal simulation delivers a point cloud representing the outer volume of a single chip from which the discrete chip geometry has to be extracted. The chip geometry can be described by the angular discretisized chip thickness h(φ,z) with the input- and exit angles $\varphi_{in}$, $\varphi_{out}$. Because the chip varies along the cutting edge the chip gets subdivided into discs of the height dz and in angular direction in dφ (cp. Figure 3).
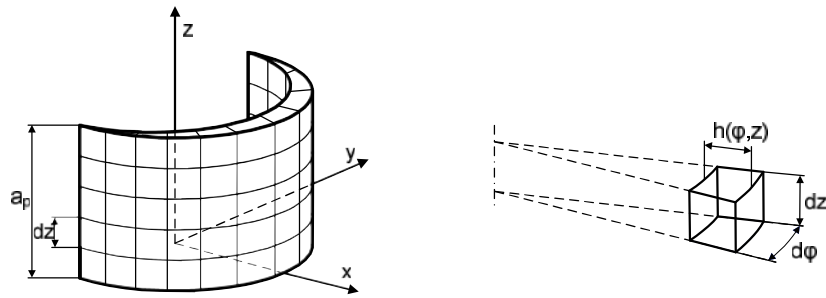
*Figure 3; Discretisiced chip geometry.*

The calculation of the chip thickness is done in three steps. In the first step the point cloud is subdivided into disks of the height dz. As a next step, inside of each disc the maximum angular points are defined as restricting points by $\varphi_{in}$ and $\varphi_{out}$ (cp. Figure 4a). Due to the complex contact conditions and hence the complex chip geometries the input and exit angles varies over the cut of depth $a_p$. The analytic chip geometry of each disk can be calculated based on the cylindrical form of the cutter at the discrete time of $t(i)$ and $t(i-1)$. The area between the input angle $\varphi_{in}$ and exit angel $\varphi_{out}$ is discretized into multiple subareas with the angular distance $d\varphi$. The value of the discrete chip thickness $h(\varphi,z)$ in respect of $\varphi$ can be calculated by a line intersection with the two cylinders in the final step (cp. Figure 4b).
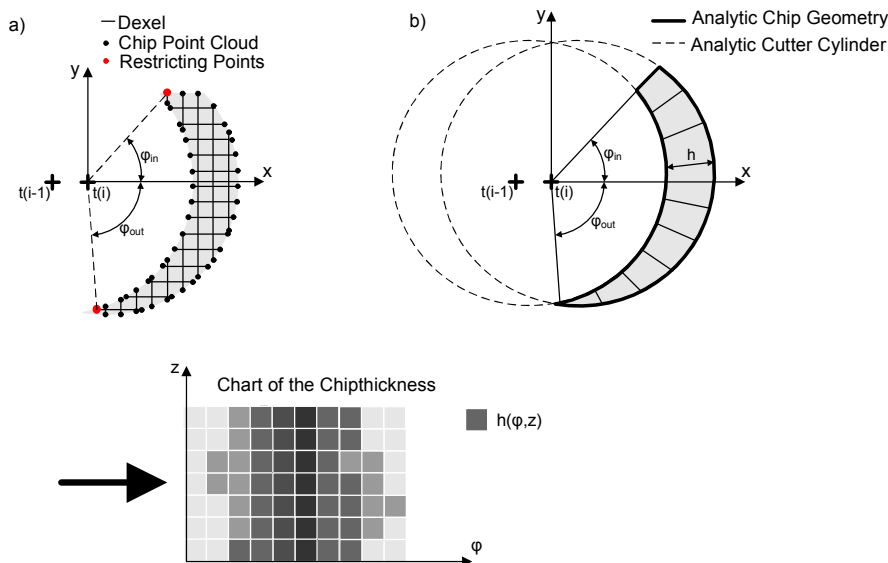


*Figure 4; Calculation of the chip thickness $h(\varphi,z)$.*

Adding all disc levels together a chart of the chip thickness $h(\varphi,z)$ can be extracted, which builds the bases of the force calculation. This is the most performed arithmetic operation during the removal simulation.

### 3.2. Cutting force model

For the prediction of the cutting forces a standard cutting force model based on Altintas is used, where the time delay responsible for the chatter is neglected [Altintas, 2000]. According to the chip discretisation the cutter is sectioned into discs of the height dz.
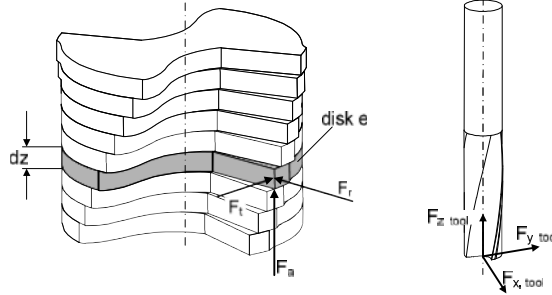


*Figure 5; Calculation of the chip thickness h(φ,z).*

In each disc e, $F_{rta,j,e}$ represents the force per tooth j in radial, tangential and axial direction.

$$F_{rta,j,e} = K_c \cdot dz \cdot h_j(\varphi,z) + K_e \cdot dz \tag{4}$$

Depending of the angular position of the tooth of one disk the corresponding chip thickness h(φ,z) is inserted. The cutting force coefficients $K_c = [K_{rc}, K_{tc}, K_{ac}]$ and $K_r = [K_{re}, K_{te}, K_{ae}]$ need to be identified in advance.

After transforming $F_{rta,j,e}$ with T(φ) and the adjacent sumation over all teeth $N_z$ and all disks $N_e$ the force $F_{xyz, tool}$ can be calculated in a non rotating tool coordinate system.

$$F_{xyz,tool} = \sum_{e=1}^{N_e} \sum_{j=1}^{N_z} T_j(\varphi) \cdot F_{rta,j,e} \tag{5}$$

The force $F_{xyz,tool}$ builds the interface to the robot model.

### 3.3. Experimental validation of the process force simulation

The computational accuracy of the process force simulation is tested without considering the robot model. The milling of a sample work piece is shown in Figure 6.
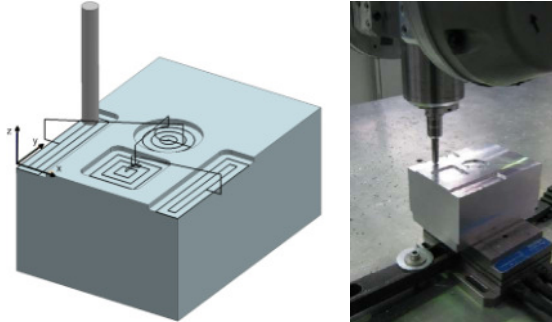


*Figure 6; CAD-Model of the used work piece (left) and the milling test setup (right).*

The machining operation starts at the right rectangle continues at the square pocket and the circle pocket and ends at the left rectangle. The test is conducted on a Reis robot RLP16 HSC with a gantry machine structure in Aluminum 3.1325 with a two flute end mill of d = 10 mm. The feed rate is $v_F$ = 50 mm/s while the axial depth of cut ap= 1mm. The spindle speed is n = 8.000 min$^{-1}$, which is measured with an internal speed and position sensor. During the milling operation the process forces are measured with a Kistler dynamometer of type 9257A. Furthermore, the tool path was recorded by the machine internal measuring sensors for the later use as input for the process force simulation. The coefficients were experimentally determined in earlier milling tests to $K_{rc}$ = 337.3 N/mm$^2$; $K_{tc}$ = 989.8 N/mm$^2$; $K_{ac}$ = 66.9 N/mm$^2$; $K_{re}$ = 15.4 N/mm; $K_{te}$ = 3.0 N/mm; $K_{ae}$ = 4.5 N/mm.



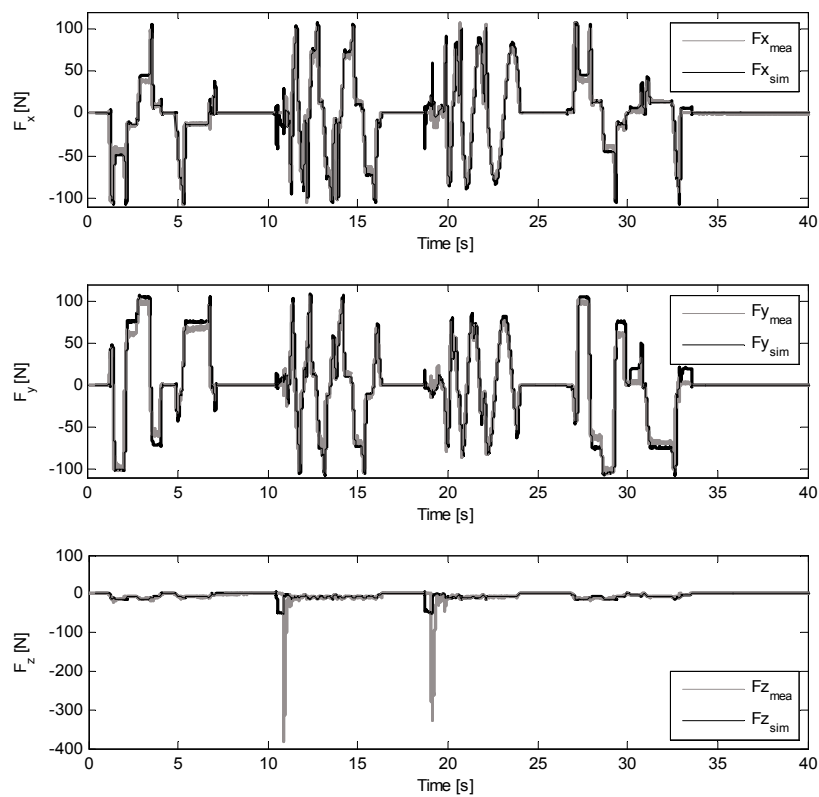*Figure 7; Measured (grey) and simulated (black) process forces in x-, y- and z-direction*

The process force simulation uses identical process parameters as in the milling experiment and the recorded tool path. The work piece dexel discretisation is set to dx = 0.2 mm, dy = 0.2 mm and dz = 0.2 mm. In Figure 7 the measured and the simulated process forces are drawn. Since the later path correction is aimed to static and low frequent oscillation of the tool path the forces are low pass filtered by a Butterworth filter with cut-off frequency of 100 Hz. The resulting quasi static process forces show a very good correlation (cp. Figure 7). Slight offsets in Fx and Fy can be observed, where the measured force is always lower than the simulated force. The reason is the

neglecting of the mechanical structure in the simulation, while in the experiment the mechanical structure was deviated slightly. The strong peaks in Fz of the measurement represent the dipping operation of the cutter. Currently, this cannot be simulated with the process force model.

## 4. SIMULATION OF THE ROBOT'S MOTION

In order to predict the static deviation during the milling process the process force model needs to be coupled with the mechanical robot structure. The robot is modeled as a chain- or tree-structured multi body system (MBS) with elasticities in the revolute joints. Forces resulting from the drives of the robot's joints are applied to the joints of the MBS, forces $F_{xyz,tool}$ resulting from the process force simulation are applied to the TCP.

### 4.1. Modeling of the multi body system

The general dynamics of a tree structured multi body system with $m$ degrees of freedom can be described with the equation

$$M(q)\ddot{q} + C(q,\dot{q}) + G(q) = \tau + S(F_{xyz,tool}, q) \tag{6}$$

with $M \in R^{mxm}$ being the inertia matrix, $C \in R^m$ being the coriolis and centrifugal forces and $G \in R^m$ being the gravitational forces [Craig, 1989]. The forces/torques resulting from the joints' drives are described by $\tau \in R^m$ and $S(F,q) \in R^m$ are the forces/torques in the joints resulting from external forces attacking at the robots tool. The joints' positions, velocities and accelerations are described by $q$, $\dot{q}$ and $\ddot{q} \in R^m$. Instead of explicitly deriving equation (6) for a specific robot, a modular approach for describing the robot is used. In this approach the robot's tree structure is described by a set of structural elements consisting of a fixed base, fixed rotations, revolute and prismatic joints and rigid bodies. For tree structured robots further on forks can be added to the structure at any point. Similar approaches have been used successfully for industrial manipulators [Höpler, 2004], biomechanical systems [Stelzer, 2007] and mobile robots [Friedmann, 2009].

As no information is available on the control strategy used in the robots motors, the drivetrain is modeled using the assumption, that the drive side angle $\theta_i$ and velocity $\dot{\theta}_i$ always are at the values desired by the path planning system. Further on it is assumed that the drive side is coupled by spring and damper system to the respective joint axis. The resulting torque $\tau_i$ for the $i$-th joint is determined by

$$\tau_i = K_i(\theta_i - q_i) + D_i(\dot{\theta}_i - qd_i) \tag{7}$$

with $K_i$ being the spring stiffness and $D_i$ being the damping.

### 4.2. Solving the equations of motion

To calculate the accelerations of the robot's joints resulting from $\tau$ and $F_{xyz}$, equation (EQ2) has to be solved. Currently the Composite-Rigid-Body-Algorithm (CRBA) [Walker and Orin, 1982; Featherstone, 2008] is used for this purpose. Without changing the modeling of the robots structure alternatively the Articulated-Body-Algorithm (ABA) [Featherstone, 1983] can be used. In [Featherstone, 2008] it is shown, that the CRBA performs better for robots with few joints, while the ABA perform better for robots with many joints (the actual break even depends on the implementation).

### 4.3. Implementation

Modelling of the robot, solving the equations of motion and numerical integration has been implemented in an object-oriented C++ class library. This class library can be interfaced from Matlab for coupling with other parts of the simulation (e.g. the process force simulation and the simulation of the drivetrain). The simulation can be used for any tree-structured robot without the need to derive equation (6) explicitly. Unlike the widely used Denavit-Hartenberg-formalism, the robot's structure is not limited to a series of links, each consisting of a revolute (or prismatic) joint followed by a rigid body and a fixed rotation. Instead, the structural elements can be combined in any order, thus allowing the integration of additional joints anywhere in the robot's structure. This feature will be used to model additional elasticities as "virtual" joints in the robots structure. To maintain an optimal runtime performance, an implementation of the ABA will be added to the existing implementation of the CRBA, thus allowing to choose the best performing solver depending on the current robot.

### 4.4. Validation of the coupled robot - process force simulation

In Figure 8 a coupled simulation of the test work piece (cp. Figure 6) is shown. The mechanical parameters of the robot model describe a Reis serial robot RV 130. The input tool path is the measured tool path of the experiment in chapter 3.3.

The Figure shows the surface dexels of the work piece, which are machined. Additionally, the desired and the simulated path are shown. In order to visualize the results only z-dexels were plotted in high scaling factor in z. It can be seen, that the surface is very wavy. Especially in the corners contour failures occur by unwanted immerging/lifting of the robot into/out of the material. This happens due to the inertia and elasticity's of the robot model. Furthermore, the simulated path shows a static offset of about 0.1 mm in z direction because of the acting process force. A similar behavior is shown in Zoom 2, where only x- and y- dexels are plotted in a strong x scaling factor. The contour failure of the work piece and the static offset is also about 0.1 mm.
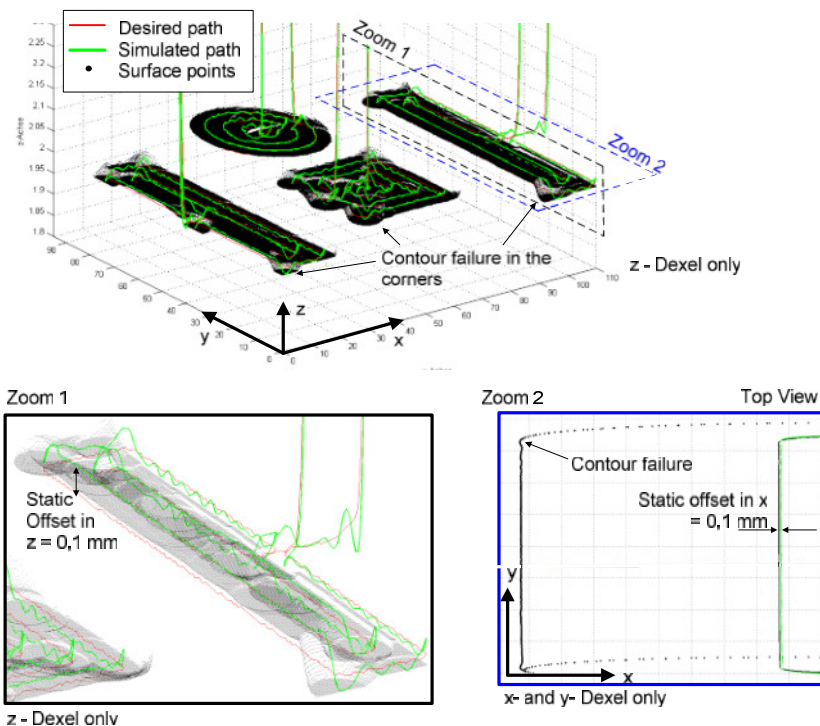
*Figure 8; Coupled Simulation of robot model and process force model.*

## 5. SUMMARY AND OUTLOOK

In this paper the implementation of a material removal simulation with an integrated cutting force model is presented. The accuracy of the process force simulation was verified by a milling test. By coupling the simulation with a robot model, the resulting TCP displacement of the robot path can be predicted. The robot model and the dynamic robot simulation is not limited to a specific type of robot, but can be used for any tree structured system. In a next step orthogonal virtual joints and elasticities are added to the object-oriented C++ robot model. Thereby a more precise deviation of the tool path will be predictable. On this basis the robot tool path can be adjusted to improve the milling quality.

REFERENCES

**[Abele et. al, 2008]** Abele, E; Bauer, J; Rothenbücher, S.; Stelzer, M.; Stryk, O.; "Prediction of the Tool Displacement by Coupled Models of the Compliant Industrial Robot and the Milling Process"; Conference on Process Machine Interaction, Hannover; 2008

**[Altintas, 2000]** Altintas, Y.; "Manufacturing Automation: Metal Cutting Mechanics, Machine Tool Vibrations and CNC Design"; Cambridge University Press; 2000

**[Craig, 1989]** Craig, J. J.; "Robotics"; Addison-Wesley; 1989

**[Featherstone, 2008]** Featherstone, R.; "Rigid Body Dynamics Algorithms"; Springer; 2008

**[Friedmann, 2009]** Friedmann, M.; "Simulation of Autonomous Robot Teams with Adaptable Levels ob Abstraction"; PhD Thesis TU Darmstadt; 2009

**[Höpler, 2004]** Höpler, R.; "A unifying object-oriented methodology to consolidate multibody dynamics computations in robot control"; PhD Thesis TU Darmstadt; 2004

**[Rehling, 2003]** Rehling, S.; Technologische Erweiterung der Simulation von NC-Fertigungsprozessen"; PhD Thesis Universität Hannover; 2009

**[Selle, 2003]** Selle, J.; Technologiebasierte Fehlerkorrektur für das NC-Schlichtfräsen"; PhD Thesis Universität Hannover; 2005

**[Surmann, 2005]** Surmann, T.; Geometrisch-physikalische Simulation der Prozessdynamik für das fünfachsige Fräsen von Freiformflächen"; PhD Thesis TU Dortmund; 2005

**[Stautner, 2005]** Stautner, M.; "Simulation und Optimierung der mehrachsigen Fräsbearbeitung"; *PhD Thesis TU Dortmund*, ; München 2002; ISBN 3-8027-8732-3

**[Stelzer, 2007]** Stelzer, M.; "Forward Dynamics Simulation and Optimization of Walking Robots and Humans"; PhD Thesis TU Darmstadt; 2007

**[Walker et. al, 1982]** Walker, M. W.; Orin, D. E.: "Efficient Dynamics Computer Simulation of Robotic Mechanisms"; In: Journal of Dynamic Systems, Measurement, and Control 104, pp. 205-211; 1982

**[Weigold, 2008]** Weigold, M.; "Kompensation der Werkzeugabdrängung bei der spanenden Bearbeitung mit Industrierobotern"; PhD Thesis TU Darmstadt; 2008; ISBN 978-3-8322-7178-7

**[Weinert et al., 2002]** Weinert, K.; Müller, H.; Kreis, W.; Surmann, T.; Ayasse, J.; Schüppstuhl, T.; Kneupner, K.; "Diskrete Werkstückmodellierung zur Simulation von Zerspanprozessen"; In: Zeitschrift für wirtschaftlichen Fabrikbetrieb: ZWF, pp. 385-389; München 2002; ISSN 0932-0482

**[Weinert et al., 2004]** Weinert, K.; Surmann, T. ; Damm, P. ; "Real Time Solid Modelling of the Milling Process"; In: Production Engineering: Research and Development; Annals of the German Academic Society for Production Engineering ; 11/2, pp. 135-138 ISSN 0944-6524